

Spinodal Decomposition in Solid Isotopic Helium Mixtures

M. Poole, J. Saunders, and B. Cowan*

Millikelvin Laboratory, Royal Holloway University of London, Egham, TW20 0EX, United Kingdom

(Received 28 July 2006; published 20 September 2006)

We report the first observations of spinodal decomposition in solid helium isotopic mixtures, using NMR measurements. The experiments were performed at a ^3He concentration of 50% where the transition proceeds through the critical point. We used an initial pressure such that the system remained solid. Our observations indicate that the transition occurs by the mechanism of spinodal decomposition and we are able to study its evolution in real time.

DOI: 10.1103/PhysRevLett.97.125301

PACS numbers: 67.80.Jd, 68.35.Rh

The phenomenon of phase separation in binary mixtures has many important practical applications, underlying the understanding of such things as the properties of polymers [1,2] and the strength of metallic alloys [3]. It also provides an ideal example of a first order phase transition with a rich parameter space, modeling systems from the early universe [4] to the crystallization of proteins [5]. Helium and helium isotopic mixtures have provided model systems for the study of phase transitions, including the lambda transition, the liquid-gas critical point and the tricritical point [6]. In these cases there has been very good agreement between theory and experiment—both phase diagram topology [6,7] and transition kinetics [8,9]. And phase separation studies in solid helium mixtures have proved rather fruitful, as the segregation process occurs on a particularly convenient time scale: slower than that in fluids, but faster than that in conventional solids. This is a consequence of the unique nature of the atomic motion in solid helium. Quantum exchange has the effect of delocalizing the atoms from their lattice sites, resulting in a diffusion coefficient intermediate between that of a solid and a liquid, and depending on pressure [6].

Central to a first order phase transition is the existence of an energy barrier separating the initial and nascent phases. Thermal fluctuations provide the energy to surmount the barrier and nucleate new-phase embryos, which then grow into the new-phase regions. This is the conventional nucleation-growth mechanism for first order transitions [10]. Homogeneous nucleation has been observed in isotopic mixtures of both solid [9] and liquid [8] helium. At a critical point the distinction between the two phases disappears; the energy barrier between the two vanishes. Away from the critical point the energy barrier may also vanish if the system is supercooled through a metastable state. When the energy barrier vanishes, phase separation becomes a *spontaneous* process, proceeding through growing spatial modulation of the order parameter; this is the mechanism of spinodal decomposition [11].

Most experimental research on phase separation and spinodal decomposition has been performed on metal alloys and in polymer mixtures. Many such experiments

have involved separately preparing specimens and then studying them; few have involved real-time investigations. The prototypical metal system is the Al-Zn alloy; this has been studied in real time by Mainville *et al.* [12] using small-angle x-ray scattering on critical mixtures. And polymer mixtures have been studied in real time by the Higgins group using light scattering, neutron scattering, and more recently atomic force microscopy [1,2]. In this Letter we report the first observation of spinodal decomposition in solid helium mixtures. These are real-time observations; using NMR we have followed the evolution of the spatial distribution of ^3He concentration upon cooling through the critical point.

Upon cooling, a solid solution of ^3He and ^4He will separate into regions rich in ^3He and regions rich in ^4He . This is a prototypical example of a first order phase transition, with a conserved order parameter. The processes occur over measurable time scales so we can study the dynamics of the transition. Moreover the system is clean, with no impurities. We grow crystals at constant pressure, which achieves specimens of high crystallographic quality [13]. The initial determination of this system's phase diagram was made by Edwards *et al.* [14] through heat capacity measurements. The phase diagram comprises three distinct regions as shown (in outline [15]) in Fig. 1: a stable (homogeneous) region *h*, a metastable region *m* and an unstable region *u*. These are separated by the

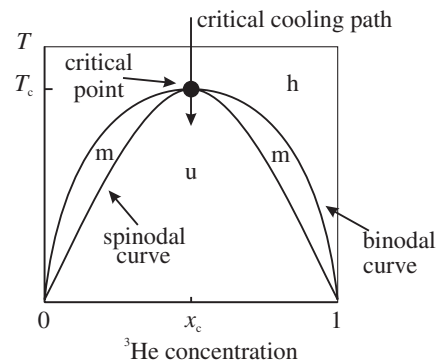


FIG. 1. Schematic features of solid mixture phase diagram.

binodal line and the spinodal line, as shown in the figure. These features of the phase diagram may be understood [16] from a free energy density $f(x)$ which is a function of the ^3He concentration x . The binodal line is determined from $\partial f/\partial x = 0$, while the spinodal line satisfies $\partial^2 f/\partial x^2 = 0$. The binodal line maps out the equilibrium coexistence states of the system. Upon cooling through the binodal line into the metastable region, phase separation requires nucleation of the new phase through thermal fluctuations in concentration. However with rapid/deep temperature quenches one can pass right through the metastable region to the unstable region. And in this case phase separation may evolve through spinodal decomposition [11,17] rather than the more common nucleation-growth process [9]. In this Letter we concentrate on studies where the system is cooled through the critical point, as shown in Fig. 1. The binodal and the spinodal lines meet at the critical point. Thus passing through the critical point allows entry directly to the unstable region from the homogeneous region.

The segregation process may be understood from elementary thermodynamic arguments. The key point is that particle flow is driven by gradients in the chemical potential, Fick's law: $\mathbf{J} = -A\nabla\mu$ in the linear régime, where A is a constant. (This behavior may not always correspond to conventional diffusion for which chemical potential is proportional to concentration). The kinetics of the process are then described by the Cahn-Hilliard equation [11]

$$\frac{\partial x}{\partial t} = A \frac{\partial^2 f}{\partial x^2} \nabla^2 x + 2A\kappa \nabla^4 x. \quad (1)$$

Here κ is the stiffness coefficient, the gradient-square term in the free energy density. This accounts for the increase in free energy density from the spatial variation of the concentration. In the absence of the stiffness term this corresponds to a conventional diffusion equation with an effective diffusion coefficient $D_{\text{eff}} = A\partial^2 f/\partial x^2$. Since the spinodal line corresponds to the change in sign of $\partial^2 f/\partial x^2$ this indicates a *negative* effective diffusion coefficient in the spinodal region. Here the smallest concentration fluctuation will lower the free energy. In other words the system is unstable against such fluctuations and atoms will be driven from regions of low concentration to regions of high concentration: reverse diffusion. This is spinodal decomposition.

During spinodal decomposition the system evolves through a continuous change in ^3He concentration; equilibrium thermal fluctuations in composition become magnified, leading to a spatial modulation of the ^3He concentration. Fluctuations of different wavelength, however, evolve at different rates. Long wavelength variations grow more slowly because the atoms have to travel larger distances. And short wavelength fluctuations grow more slowly, inhibited by the cost in interfacial energy. Solution of the (linearized) Cahn-Hilliard equation gives

$$\Delta x(\mathbf{r}, t) \sim \cos(\mathbf{k} \cdot \mathbf{r}) \exp[R(k)t], \quad (2)$$

where $R(k)$ is the amplification factor for the fluctuations of wave vector \mathbf{k}

$$R(k) = -D_{\text{eff}} k^2 \left[1 + 2\kappa k^2 \left(\frac{\partial^2 f}{\partial x^2} \right)^{-1} \right]. \quad (3)$$

There is thus an optimum intermediate length scale λ_{opt} , or wave vector $k_{\text{opt}} = 2\pi/\lambda_{\text{opt}}$, for which the fluctuations grow most effectively. This corresponds to the maximum in $R(k)$, so that

$$\lambda_{\text{opt}} \sim \sqrt{\kappa/|\partial^2 f/\partial x^2|} \quad (4)$$

and λ_{opt} diverges at the critical point.

The power of NMR in studies of phase separation in helium mixtures is due to the dependence of the relaxation times T_1 and T_2 on ^3He concentration. The NMR signal is from the ^3He alone, the signal size being proportional to the ^3He magnetization. The relaxation times depend on the strength of the internuclear dipolar fields and on their time modulation [18]. Both of these depend on the ^3He concentration [19]. Thus two coexisting phases will give a two-component NMR signal from which the two relaxation times and intensities may be found [20]. This has been utilized in our previous studies, away from the critical point [20], where the phase separation transition is manifest in the sudden appearance of a new and distinct NMR signal components in both T_1 and T_2 measurements.

The situation is different when the transition proceeds through the critical point. Then the spatial variation of ^3He density results in a (continuous) spatial variation of relaxation rates. And such a distribution gives an NMR relaxation profile qualitatively different from the two components observed for two coexisting phases, when one cools into the metastable region.

We report measurements on a crystal comprising a 50% mixture of ^3He and ^4He . In order to ensure good crystallographic quality the crystal was grown at constant pressure; x-ray measurements have shown this method to produce crystals of high quality [13]. The procedure has been described elsewhere [9]. However, because of the relatively large separation of the liquidus and the solidus curves of the 50% mixture [21], it was necessary to grow the crystal very slowly (~ 15 h) to ensure homogeneity. Crystal growth and homogeneity were monitored continuously using NMR [9]. Following crystal completion the specimen was annealed at 1.4 K, close to the melting point, to enhance homogeneity and remove crystalline imperfections. The final pressure of the homogeneous mixture was 36.7 bar.

In initial experiments on this crystal the temperature was lowered in small temperature steps ~ 5 mK. This enabled us to determine the critical temperature of the crystal to be 400 mK from both pressure and NMR measurements; the pressure increases when segregation commences [9,22].

During detailed studies of phase separation the temperature was reduced in larger steps ~ 20 mK. The main NMR data recorded was the transverse relaxation.

A typical spin echo relaxation following a 90° - τ - 180° -echo sequence is shown in Fig. 2. Observe that the data cover over $3\frac{1}{2}$ decades of amplitude. This is an extremely large dynamic range by NMR standards exceeded, probably, only by Engelsberg and Lowe [23]. Special care must be taken with instrument calibration when capturing data over such a range.

Spinodal decomposition involves the spatial variation of ^3He density and this results in a continuous variation of relaxation rates. If $g(s)$ is the distribution function of transverse relaxation rates $s = T_2^{-1}$ then the normalized spin echo relaxation profile $f(t)$, is given by the superposition of decaying exponentials:

$$f(t) = \int_0^\infty g(s)e^{-st} ds, \quad (5)$$

the Laplace transform of the distribution function.

We observed that the nonexponential relaxation profile, found upon cooling through the critical point directly into the spinodal region, was found to follow a stretched exponential function [24]

$$f(t) = e^{-(\alpha t)^n}, \quad (6)$$

where α is an effective relaxation rate and n is an index with values between 0 and 1. Such a relaxation, also known as a Kohlrausch-Williams-Watts function, occurs frequently in the description of such diverse phenomena as earthquakes, stock markets, galactic light emission, biological extinction, and NMR in inhomogeneous systems such as cream cheese [25] (and references therein).

We emphasize that the adoption of the stretched exponential profile is but a convenient parameterization of the experimental data although we note that this function emerges, in a ‘‘central limit’’ sense, as the characteristic function of distributions with divergent second moments

[26]. Within this picture the index n gives a measure of the spread in the range of contributing relaxation rates. Thus $n = 1$ corresponds to a single relaxation rate—no spread—while decreasing values of n indicate an increasing spread of relaxation rates [27].

The echo relaxation data were fitted to the stretched exponential function to determine the initial amplitude, the effective relaxation rate α and the index n . Above the critical temperature the index was unity, indicating the single-component signal of a homogeneous crystal. The first step through the transition was to a temperature of 379 mK, a decrement of 21 mK. The subsequent evolution of the echo relaxation was monitored over a period of ~ 275 h. The behavior of the inhomogeneity index n is shown in Fig. 3.

Initially, upon cooling through the critical point, the index dropped from unity to 0.835 over a period of about 20 h. We interpret this to indicate that during this period a growing multiplicity of relaxation rates (concentrations) evolves, identified through the drop in n . As the system evolves further, over a much slower time scale, the index then rises steadily. This indicates the range of contributing relaxation rates decreasing. This occurs as the system evolves to its equilibrium configuration, a coexistence of regions of two different concentrations, as determined from the binodal (phase separation) curve Fig. 1 of the phase diagram.

Cahn and Hilliard [11] address the question of how to distinguish experimentally between spinodal decomposition and the nucleation or growth process. They state that spinodal decomposition should possess the following properties: (1) it should occur everywhere within the specimen; and (2) the amplitude of composition fluctuations should grow continuously until a metastable equilibrium is reached with a preferential amplification of certain wavelength components.

It is clear that condition (1) is satisfied since the relaxation profile fits so well to the stretched exponential func-

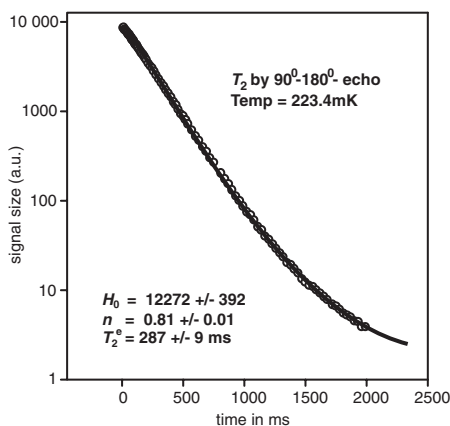


FIG. 2. Typical spin echo relaxation data together with stretched exponential fit.

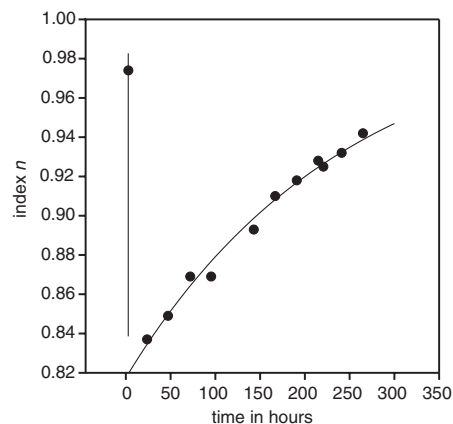


FIG. 3. Evolution of stretched exponential index n following cooling through the critical point.

tion. From the general form of the inverse Laplace transform of this function, it indicates that the concentration variations have a smooth and unimodal distribution function.

Considering condition (2), the drop in n from \sim unity to its minimum value indicates the amplitude of composition fluctuations growing continuously. The minimum corresponds to the metastable equilibrium. Then, following this, the smooth spatial variation evolves into distinct high- and low-concentration regions.

Scattering experiments measure the structure factor $S(\mathbf{k}, t)$, the autocorrelation function of the concentration fluctuations. From the Cahn-Hilliard equation it follows [1] that

$$S(\mathbf{k}, t) = S(k, 0) \exp[2R(k)t], \quad (7)$$

where $R(k)$ is the fluctuation amplification factor described earlier. Although our NMR measurements are unable to determine directly the spatial variation of the composition or the dominant wavelength of the composition variation, there is an indirect way in which the dominant length scale of the composition variations may be estimated. The increase in the index n in Fig. 3 reflects the evolution of the equilibrium two-phase state as the ^3He atoms travel out of the ^4He -rich regions and *vice versa*. The solid line in this figure is a least squares fit of an exponential curve and this gives the time constant τ for the process to be ~ 250 h or $\sim 10^6$ s. If the diffusion coefficient of this transport is D then in this time atoms will travel a distance $\sim (D\tau)^{1/2}$. Then taking the diffusion coefficient for this mixture to be $\sim 10^{-10} \text{ cm}^2 \text{ s}^{-1}$ [9], this gives a length scale of the order of 10^{-4} m, comparable with the length scales observed, by both light scattering and by atomic force microscopy, in spinodal decomposition in polymer mixtures of $\sim 10^{-5}$ m [1].

We have shown that, at the critical point, phase separation in solid helium mixtures proceeds through spinodal decomposition. We have used NMR to follow the evolution of the distribution of ^3He concentrations through analysis and interpretation of the spin echo relaxation profiles in terms of a stretched exponential function.

The authors wish to acknowledge helpful discussions with Tom Crane, Mihail Fardis, and Ian Ford. Financial support from the EPSRC is gratefully acknowledged.

*Electronic address: b.cowan@rhul.ac.uk

[1] J. T. Cabral, J. S. Higgins, T. C. B. McLeish, S. Strausser, and S. N. E. Magonov, *Macromolecules* **34**, 3748 (2001).

- [2] J. T. Cabral, J. S. Higgins, N. A. Yerina, and S. N. E. Magonov, *Macromolecules* **35**, 1941 (2002).
- [3] D. McKie and C. McKie, *Crystalline Solids* (Nelson, London, 1974).
- [4] G. E. Volovik, *The Universe in a Helium Droplet* (Oxford, New York, 2003).
- [5] P. G. Debenedetti, *Nature (London)* **441**, 168 (2006).
- [6] K. H. Bennemann and J. B. Ketterson, *The Physics of Liquid and Solid Helium* (Wiley, New York, 1976).
- [7] D. O. Edwards and S. Balibar, *Phys. Rev. B* **39**, 4083 (1989).
- [8] P. Alpern, T. Benda, and P. Leiderer, *Phys. Rev. Lett.* **49**, 1267 (1982).
- [9] A. Smith, S. Kingsley, V. A. Maidanov, E. Y. Rudavskii, V. N. Grigorev, V. V. Sleзов, M. Poole, J. Saunders, and B. Cowan, *Phys. Rev. B* **67**, 245314 (2003).
- [10] J. W. Cahn and J. E. Hilliard, *J. Chem. Phys.* **28**, 258 (1958).
- [11] J. W. Cahn, *Acta Metall.* **9**, 795 (1961).
- [12] J. Mainville, Y. S. Yang, K. R. Elder, and M. Sutton, *Phys. Rev. Lett.* **78**, 2787 (1997).
- [13] B. A. Fraass and R. O. Simmons, *Phys. Rev. B* **36**, 97 (1987).
- [14] D. O. Edwards, A. S. McWilliams, and J. G. Daunt, *Phys. Rev. Lett.* **9**, 195 (1962).
- [15] This simplification ignores the hcp to bcc transition that occurs in the vicinity of $x_3 \sim 0.1$; the actual details of the ^3He - ^4He phase diagram, including this feature, are treated by Edwards and Balibar [7].
- [16] J. C. Slater, *Introduction to Chemical Physics* (Dover, New York, 1970).
- [17] J. W. Cahn and J. E. Hilliard, *J. Chem. Phys.* **31**, 688 (1959).
- [18] B. Cowan, *Nuclear Magnetic Resonance and Relaxation* (Cambridge University Press, Cambridge, England, 1997).
- [19] A. S. Greenberg, W. C. Thomlinson, and R. C. Richardson, *J. Low Temp. Phys.* **8**, 3 (1972).
- [20] S. Kingsley, V. Maidanov, J. Saunders, and B. Cowan, *J. Low Temp. Phys.* **113**, 1017 (1998).
- [21] P. M. Tedrow and D. M. Lee, *Phys. Rev.* **181**, 399 (1969).
- [22] W. J. Mullin, *Phys. Rev. Lett.* **20**, 254 (1968).
- [23] M. Engelsberg and I. J. Lowe, *Phys. Rev. B* **10**, 822 (1974).
- [24] G. Williams and D. C. Watts, *Trans. Faraday Soc.* **66**, 80 (1970).
- [25] E. R. Hunt, P. M. Gade, and N. Mosseau, *cond-mat/0204179*.
- [26] E. W. Montroll and J. T. Bender, *J. Stat. Phys.* **34**, 129 (1984).
- [27] We have shown, by mathematical modeling, how a sinusoidal distribution of relaxation rates leads to an approximately stretched exponential profile. This demonstrates, in particular, how the index n relates to the spread of the distribution.